Tyrosine 162 of the Photosynthetic Reaction Center L-Subunit Plays a Critical Role in the Cytochrome c_2 Mediated Rereduction of the Photooxidized Bacteriochlorophyll Dimer in *Rhodobacter sphaeroides*. 2. Quantitative Kinetic Analysis

J. Wachtveitl, J. W. Farchaus,‡ P. Mathis,§ and D. Oesterhelt*

Department of Membrane Biochemistry, Max Planck Institute for Biochemistry, am Klopferspitz 18a, 82143 Martinsried, Germany

Received April 15, 1993; Revised Manuscript Received July 20, 1993®

ABSTRACT: The electron-transfer kinetics from the soluble cytochrome (cyt) c_2 to the photooxidized reaction center (RC) was studied with proteins isolated from *Rhodobacter* (*R.*) *sphaeroides*. In addition to wild-type (WT) RC, RCs harboring site-directed mutations at residue L162 (L162F, -M, -L, -S, or -G) were analyzed. The disappearance of the absorption band of the photooxidized primary donor P^+ (at 1250 nm) and the α-band of cyt c_2 (at 550 nm) were monitored. Under conditions of high equimolar RC and cyt c_2 concentrations, the kinetics were very similar to those measured in intact cells (Farchaus et al., 1993). The fast component of the kinetics normally seen in WT was not observed in any of the mutants; the overall rereduction rates for the mutants depended on the amino acid substitution. Light intensity, viscosity, ionic strength, and RC/cyt c_2 stoichiometry of the reaction mixture were varied to distinguish the contributions of association, reorientation, and electron-transfer reactions to the observed kinetics. In competition experiments, WT RC (L162Y) and the mutant RC L162L showed similar affinity for cyt c_2, with a dissociation constant of $k_D = 10^{-6}$ M. Mutants with an aliphatic substitution at position L162 displayed slower cyt c_2–RC association and dissociation rates. Comparison of the major kinetic component of the P^+ rereduction rates for the aliphatic substitutions to the aromatic substitution, L162F, revealed that the former were less affected by ionic strength and viscosity than the latter. The viscosity and ionic strength dependences noted for L162F were comparable to those seen for the slow kinetic component observed for the WT RC. The redox midpoint potential of the P/P^+ couple was increased by 30 mV (L162F) to 50 mV (L162L,G) over the WT value, leading to differences in ΔG not large enough to account for the drastic kinetic effects. Rather, the results suggested that the state(s) where cyt c_2 is nonproductively bound to the RC dominated in the mutants. In the L162F mutant, it appeared that only the distribution between the bound cyt c_2 states was affected, whereas for the mutants with aliphatic substitutions, a decreased reorientation rate had to be additionally assumed in order to explain the observations.

The initial event in the conversion of light energy into chemical energy in prokaryotic photosynthesis is a charge-separation reaction which leads to the transfer of an electron from a photooxidizable primary donor to an acceptor molecule in a pigment–protein complex called the reaction center (RC).[1] A high quantum yield is achieved only when the photooxidized electron donor is rereduced more rapidly by an interprotein electron-transfer event than by the competing intramolecular charge recombination event. In the purple bacterium, *Rhodobacter* (*R.*) *sphaeroides*, cytochrome (cyt) c_2 serves as the reductant of the photooxidized bacteriochlorophyll (bchl) *a* dimer, P^+. The kinetics of this electron-transfer reaction has been analyzed in intact cells (Dutton et al., 1975), in chromatophore preparations (Bowyer et al., 1979; Overfield et al., 1979), and also in great detail with purified RCs (Overfield et al., 1979; van der Wal et al., 1987; Moser & Dutton, 1988). In each case, the reaction was found to be multiphasic, and a three-state model was proposed (Overfield & Wraight, 1980a) which describes one unbound and two bound cyt c_2 states, termed "off", "distal", and "proximal", respectively. In this model, the proximal bound cyt c_2 is responsible for the rapid rereduction of P^+, while the slower phases are attributed to the distal, or off states, which require reorientation or association reactions prior to electron donation. Analysis of the dichroism of the cytochromes responsible for the two kinetic components revealed that only the bound form causing the fast phase was dichroic, suggesting that the heme orientations of the two populations of bound cyt are physically distinct (Tiede, 1987). Further evidence for different bound states and a model describing the relationship between these states were based on the viscosity dependence of the distal to proximal transition (Moser & Dutton, 1988).

The complex kinetics observed for the interprotein electron donation between the RC and cyt is not unique. The electron-transfer events associated with other systems such as cyt peroxidase or cyt oxidase (Ferguson-Miller et al., 1978) are often bi- or multiphasic, and in many cases, the redox reactions exhibit a rapid phase [reviewed in Isied (1984)]. One common feature in each of these systems in which soluble cytochromes act as donors is that the electrostatic interaction with the membrane-bound redox partners is an important element. An asymmetric distribution of lysine residues on the cyt surface creates a strong dipole across the molecule, and experiments with charged and uncharged membranes (Overfield & Wraight, 1980a,b) support the idea of the two-dimensional diffusion of cyt along the membrane. Since the positive side

* Author to whom correspondence should be addressed.
‡ Bacteriology Division, United States Army Research Institute for Infectious Diseases, Fort Detrick, Frederick, MD 21701-5011.
§ Section de Bioénergétique, Département de Biologie Cellulaire et Moléculaire, CEN Saclay, 91191 Gif-sur-Yvette Cedex, France.
® Abstract published in *Advance ACS Abstracts*, September 15, 1993.
[1] Abbreviations: bchl, bacteriochlorophyll; bphe, bacteriopheophytin; CFU, colony-forming unit; cyt, cytochrome; LDAO, *N*,*N*-dimethyldodecylamine *N*-oxide; OG, *n*-octyl β-D-glucopyranoside; P, primary donor (bacteriochlorophyll dimer); *R*, *Rhodobacter*; RC, reaction center; *Rps.*, *Rhodopseudomonas*; WT, wild type.

0006-2960/93/0432-10894$04.00/0

of the cyt dipole axis complements the negatively charged binding domain of its redox partner (Hall et al., 1987), the cyt molecule becomes preoriented prior to binding. The complex electron-transfer kinetics observed for the interaction of cyt with the RC, cyt oxidase, or cyt peroxidase follows from the subsequent binding and/or reorientation of the positively charged cyt heme crevice domain on the negatively charged domain(s) of the redox partner.

In the accompanying article, we provide strong evidence that the residue L162Y plays a key role in defining the complex kinetics of electron donation from cyt to RC, consistent with a model placing this residue within an RC domain critical to optimal electron transfer from cyt c_2. Although the effects of mutation were clearly restricted to electron transfer between cyt c_2 and RC, the *in vivo* measurements did not allow us to distinguish between binding, reorientation, or electron-transfer phenomena. In this article, the P^+ rereduction kinetics for isolated RCs was analyzed quantitatively under a variety of conditions, and effects on docking, orientation, and electron-transfer reactions for each of the L162 mutants have been distinguished. A preliminary report on this study has been presented elsewhere (Wachtveitl et al., 1993).

MATERIALS AND METHODS

Cell Growth and Genetic Methods. Growth conditions for *R. sphaeroides* strains and construction of site-directed mutants are described in the preceding article (Farchaus et al., 1993) and in Gray et al. (1990). The plasmids carrying the mutated RC genes were introduced individually into the neurosporene accumulating *puf*Δ*LMX* deletion strain PUFΔ-LMX21/3, as described in Farchaus and Oesterhelt (1989).

Protein Isolation. Chromatophores were prepared as described in Farchaus et al. (1993); RCs were isolated using the method of successive extractions described in detail in Gray et al. (1990). Usually two extractions with 0.25% LDAO (w/v) were performed, and the second extract contained the solubilized RC protein. This solution was applied subsequently to two ion exchange columns (DEAE–cellulose DE-52, Whatman, Maidstone, England, and Fraktogel TSK DEAE-650, Merck, Darmstadt, Germany). If necessary, a final purification step was performed by using the Mono-Q column of an FPLC system (Pharmacia, Uppsala, Sweden). All preparations used in this study had a 280/803 nm absorbance ratio of 1.4 or less, indicating high purity.

For detergent exchange, the RC protein was bound to a DEAE–cellulose DE-52 column (total column volume 1-2 mL) which was equilibrated with 20 mM Tris-HCl (pH 8). The column was washed with 100 mL of 20 mM Tris-HCl (pH 8) and 0.8% (w/v) octyl glucoside (OG), and the RC was eluted with 10 mL of the same buffer containing 400 mM NaCl.

If further concentration of the protein samples was required, Centricon 100 concentrators equipped with a YM 100 membrane (Amicon, Beverly, MA) were used.

Concentrated RCs were dialyzed for 12-15 h at 4 °C against a minimum 100-fold volume of 20 mM Tris-HCl (pH 8) containing the corresponding detergent [0.08% (w/v) LDAO or 0.8% (w/v) OG].

Proteoliposomes containing L162F RCs used in the electrochemical redox titrations were prepared according to the method described by Gabellini et al. (1989). The ratio of RC to ubiquinone-10 to phospholipid was 1:50:1000; the final RC concentration was 12.5 μM. Insertion of RC into the preformed liposomes was achieved by sonicating twice for 5 s. Incorporation was tested by the addition of an anionic fluorescent membrane label to the solution and then sucrose density gradient centrifugation, which yielded a band containing both the RC (tested by the absorbance spectrum) and the fluorescent probe.

Native cyt c_2 was isolated from *R. sphaeroides* WT ATCC 17023 cells according to the method described by Bartsch (1971), with the modification that the ammonium sulfate precipitation step was omitted. A total of 27 mg cyt c_2 with an absorbance ratio of $A_{275nm}^{(ox)}/A_{416nm}^{(red)} = 0.22$ was obtained from 200 g of cells (wet weight).

Electrochemical Redox Titration. The cuvette used for redox measurements was a modified version of the thin-layer cell used earlier (Hawkridge & Ke, 1976; Smith et al., 1981) for electrochemical titrations of biological electron carriers. The optical path length of the custom-made quartz cuvette (fabricated by Hellma, Müllheim, Germany) was 0.2 mm, and the sample volume was 0.6 mL. For the working electrode, an optically transparent gold mesh (50% transmittance, 500 lines/in., Buckbee-Mears Co.) was glued onto a frame of mylar foil to improve the rigidity of the gold grid. A platinum wire was threaded and glued to the top of the gold grid. The counter electrode was constructed from a platinum wire and, the reference electrode was a Ag/AgCl electrode filled with 1 M KCl as the electrolyte solution. The measurements were performed at 20 °C using a potentiostat (EG&G Princeton Appl. Research, Princeton, NJ), and the equilibration time after each step in potential was followed by monitoring the current between the electrodes, which decayed within 15-45 min to values below 1 μA.

The light-induced absorbance changes were recorded during the oxidative part of the titration, and the remaining photobleached RC was taken as the amount of reduced P. In the following reductive part of the titration, it was confirmed that the signal could be restored to its original amplitude, and therefore no RC activity was lost during the potentiometric cycle. The sample was protected from light by a shutter that blocked the measuring beam between the individual experiments.

The redox mediators phenazine methosulfate, *N,N,N′,N′*-tetramethyl-*p*-phenylenediamine, ferricyanide (all Sigma, Deisenhofen, Germany), and porphyrexide (kind gift of A. W. Rutherford) were used at 10 μM final concentration. The RCs were in 0.8% (w/v) OG at a concentration of 12.5 μM.

Spectrophotometric Measurements. The relative amounts of oxidized/reduced RC during the potentiometric measurements were determined by steady-state photobleaching. The changes in the Q_Y region (680–1000 nm) were recorded on a photodiode array spectrophotometer (Uhl et al., 1985). The measuring beam intensity was reduced by a 1% neutral density filter and an RG 665 filter (Schott, Mainz, Germany). The changes induced by the actinic measuring light were recorded as the difference between the initial spectrum and a spectrum recorded 150 ms later.

Measurements of the light intensity dependence of the cyt c_2 to RC electron-transfer reaction were carried out using the setup described above with the modification that an SFK11 filter (λ_{max} = 547 nm, half-width 30 nm, Schott) replaced the RG 665 filter in the measuring beam, further reducing the intensity to nonactinic levels. The sample was excited at 595 nm using an excimer laser (EMG 53 MSC) pumped dye laser (FL3001, Lambda Physics, Göttingen, Germany) with Rhodamine 6B as the dye. The flash had a pulse length of approximately 10 ns, and its intensity was attenuated with neutral density filters. In these experiments, 200 data points at intervals of 0.5 ms were taken at 540 and 550 nm simultaneously.

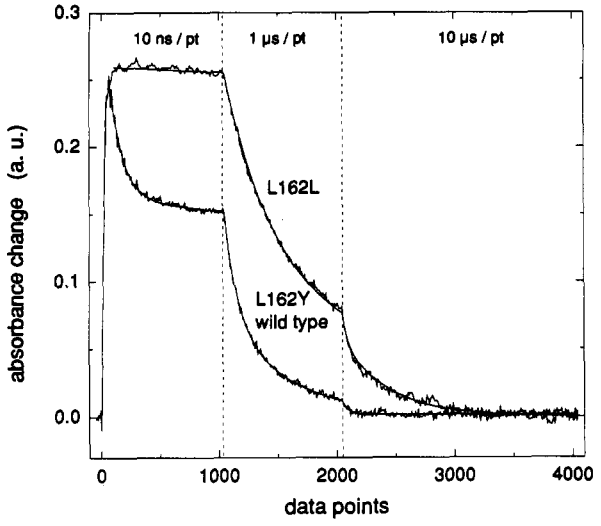

FIGURE 1: Electron-transfer reaction between isolated cyt c_2 and RCs detected at 1250 nm. The kinetics of the flash-induced absorbance changes (decay of the P^+ state) are shown for WT and the L162L mutant. The signals were obtained by averaging four single flash experiments. Excitation was provided by a 10-ns dye laser pulse at 595 nm. In both cases, RC and cyt c_2 were present at 10 µM in 20 mM Tris (pH 8.0), 0.025% LDAO, 60 µM naphthoquinone, and 100 µM ascorbate. The transients were fit to a sum of two exponentials (—).

Kinetic measurements at 1250 nm were performed on a Zeiss UMSP80 microspectrophotometer (Zeiss, Oberkochen, Germany) equipped with two Ultrafluar 10× lenses as objective and condensor. The continuous light source for the measuring beam was a 75-W xenon lamp. The light was defined before and after the sample by two broad-band interference filters (Schott) centered around 1250 nm (half-width ≈ 40 nm). A sample volume of 5-10 µL was used in a quartz cuvette with an optical path length of 1 mm. The laser beam was optically coupled to this setup via a light guide (3 mm diameter, Schoelly Optics, Danzlingen, Germany). The flash-induced absorbance changes were detected with a J-16 germanium photodiode connected to a PA-G60 preamplifier (Judson Infrared, Inc., Montgomeryville, PA). This signal was detected and stored directly with a Tektronix 2430 digitizing oscilloscope (Tektronix, Beaverton, OR). In multiple flash experiments the excitation frequency was less than 0.2 Hz. The averaged kinetic traces at this frequency showed no deviation from ones obtained in single flash experiments, indicating that the time between the flashes was sufficient to allow restoration of the Q_B site and reduction of the cyt c_2 by the added redox mediators. Since the reduction of cyt c_2 was complete in the time frame of the flash repetition, contributions from product inhibition due to oxidized cyt c_2 bound to the RC were negligible.

Fast measurements in the near infrared (Figures 1, 2, and 7; Tables I and II) were performed as described in the accompanying article (Farchaus et al., 1993), except that the signals were recorded with a transient recorder (Tektronix RTD 710 A) to facilitate the collection of data at several time resolutions from a single trace (as in Figure 1).

The ionic strengths of the solutions used for measurements at varying NaCl concentrations were monitored with a conductivity meter (WTW, Weilheim). The kinetic analysis of the absorbance transients was performed by using the Marquardt–Levenberg algorithm.

RESULTS

As shown in the accompanying article (Farchaus et al., 1993), the L162 site-directed mutants remained capable of phototrophic growth, in spite of the drastic changes in P^+ rereduction kinetics compared to WT. It could be shown *in vivo* that the fast component is missing in all of the mutants and that the rate of the slow phase is dependent on the amino acid substitution.

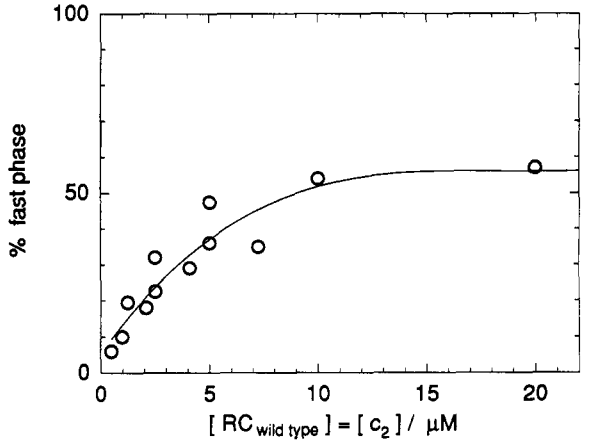

FIGURE 2: Extent of the fast phase of the RC rereduction in WT at varying equimolar concentrations of the reactants. Excitation was as in Figure 1.

Although the effects *in vivo* were localized to the electron-transfer event from cyt c_2 to RC (Farchaus et al., 1993), it was impossible to distinguish between binding, reorientation, or electron-transfer phenomena. In order to analyze the kinetics more quantitatively, RCs were isolated from each of the mutants and cyt c_2 was isolated from the parental strain. RCs were purified from semiaerobically (0.2–0.4% O_2 saturation) grown cells of the pufΔLMX deletion strain which had been complemented *in trans* with pRK404 derivatives carrying the various mutations (Farchaus et al., 1990). As described in the accompanying article, the absorption maximum in the Q_Y region of P (865 nm for WT) exhibited a hypsochromic shift (5-8 nm) in all mutant RCs; however, the intensity of this band was not affected by the mutations, and the ratio of the absorption maxima of the bchl *a* monomers to P (A_{803nm}/A_{865nm} for WT) remained 2.2 in all cases.

Experiments at RC:cyt c_2 Stoichiometry of 1. Figure 1 shows the kinetic traces for WT and the L162L mutant and the corresponding fit analysis. The reduction of the P^+ state by an equimolar amount of cyt c_2 was recorded at 1250 nm and displayed on three different time scales. The intensity of the laser flash at 595 nm was high enough to photooxidize more than 90% of the RCs. Unless stated otherwise, this extent of photooxidation was maintained throughout all the experiments described here. The WT kinetics was modeled using the sum of two exponential functions; the combination of a fast phase with a half-time of 1 µs and a slow phase with a half-time of 95 µs provided an excellent fit. Under these conditions, the two phases contributed 53% and 47% to the total amplitude, respectively. In some cases, a very slow component having a half-time of 3–10 ms was required to model accurately the kinetics of the isolated RCs. This same very slow component was routinely observed in intact cells (Farchaus et al., 1993; Dutton et al., 1975). The relative contribution of this phase was less than 10% of the total amplitude with isolated RCs.

Variation of the total protein concentration, while the 1:1 stoichiometry was maintained, led to kinetic traces for WT RCs which were also fit using two exponential functions. The fast phase (half-time 1 µs) increased in amplitude as the concentrations of both reactants were raised until a plateau of 60% fast phase was reached (Figure 2). The slow phase of the P^+ rereduction process in WT decreased in amplitude

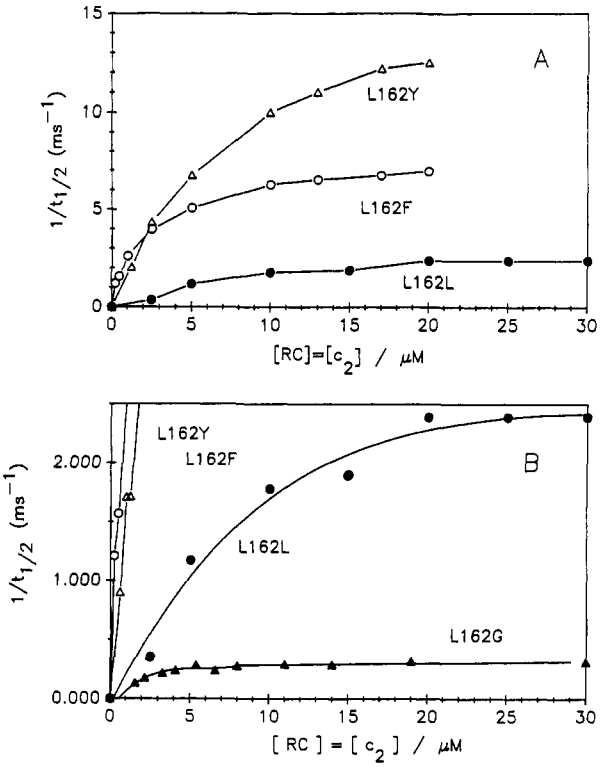

FIGURE 3: (A) Plot of inverse half-time of the P^+ reduction kinetics (for WT: slow component) vs equimolar concentration of reactants for WT, L162F, and L162L. (B) Same data presented on a time scale 6 times slower, including data for L162G.

concomitantly. In addition, the half-time decreased and reached a value of 100 μs at equimolar protein concentrations higher than 10 μM. Analysis of the slow phase in the kinetic traces at low protein concentrations revealed the expected second-order reaction, consistent with a contribution due to a bimolecular reaction of unbound cyt c_2 with the RC. At higher concentrations, a pseudo-first-order reaction was observed. The fact that the kinetics of the slow phase plateaued at 100 μs (Figure 3A, upper trace) and never approached 1 μs clearly showed that the reaction scheme is more complicated than a simple complex formation with subsequent (fast) electron transfer. As suggested earlier (Dutton et al., 1975; Overfield et al., 1979), a monomolecular transition termed "reorientation" of the docked cyt c_2–RC complex precedes the electron-transfer event and represents the rate-limiting step between docking and rapid electron transfer from cyt c_2 to P^+. The value of 100 μs reported here lies between the previously published values [55 μs, Tiede et al. (1993), 65 μs, Long et al. (1989), and 200 μs, Overfield et al. (1979)], and the overall kinetic characteristics under these conditions were so similar that the same reaction scheme had to be assumed.

For the interpretation of the kinetic data of WT, it is crucial to point out that under equimolar conditions 100% fast phase cannot be achieved and that the limit of the rate of the second component was well below the fast phase (10^4 vs 10^6 s^{-1}). Taking into account that RC–cyt c_2 complex formation is an equilibrium reaction in the dark and that P is effectively converted to P^+ by the flash, the model of Overfield et al. (1979) is indeed the minimal kinetic scheme for this reaction:

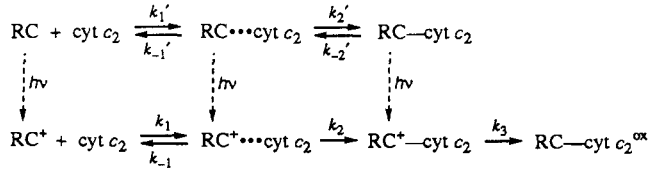

Table I: Kinetic Characteristics of the P^+ Reduction by Cyt c_2[a]

	equimolar [RC] = [cyt c_2]		excess [cyt c_2] (6.5-fold)	
	$t_{1/2}^{fast}$ (μs)	$t_{1/2}^{slow}$ (μs)	$t_{1/2}^{fast}$ (μs)	$t_{1/2}^{slow}$ (μs)
L162Y (WT)	1.0 (53%)	100 (47%)	0.8 (58%)	32 (42%)
L162F		140	3.0 (8%)	85 (92%)
L162M		nd		240
L162L		430		295
L162G		2900		820
L162S		nd		1100

[a] Two different conditions of measurement were chosen: (i) equimolar, 20 μM RC and cyt c_2 (L162G: 19 μM); (ii) excess cyt c_2, 2 μM RC and 13 μM cyt c_2. In both sets of experiments, 200 μM ascorbate and 500 μM ubiquinone UQ_6 were present. For the fast part of the reaction usually 10 absorbance change traces were averaged; for recordings on the slower time scale 2–5 traces were averaged. The relative amplitudes of the different phases are given in parentheses. The extent of the fast phase was determined after the traces were corrected for the flash artifact signal. For equimolar experiments, protein concentrations chosen were sufficient to saturate the bimolecular part of the overall reaction (see Figure 3).

The rate constants for the association [RC reduced (RC), k_1'; RC photooxidized (RC^+), k_1], dissociation (RC, k_{-1}'; RC^+, k_{-1}), reorientation (RC, k_2', k_{-2}'; RC^+, k_2), and electron-transfer steps (k_3) are denoted for the corresponding reactions.

The fast reaction phase was absent for L162L (Figure 1, upper trace) and all of the mutants investigated here. Analysis of the kinetics for L162L revealed that a single exponential component with a half-time of 560 μs and an amplitude corresponding to 90% of the total provided an excellent fit. The residual amplitude of about 10% was fit by an exponential function with a half-time between 3 and 10 ms described above as the very slow phase for WT RC preparations or intact cells.

As with the WT slow phase ($t_{1/2}$ = 100 μs), the kinetics of the mutants also exhibited a marked acceleration and an eventual plateau of rate with increasing protein concentrations under equimolar conditions. This was shown for L162F, L162L (Figure 3A) and L162G (Figure 3B), where the minimal half-times were 140 μs (L162F), 430 μs (L162L), and 2.9 ms (L162G). The results for WT and mutant proteins at 20 μM are summarized in Table I (columns 1 and 2). A fast component was resolved exclusively in WT, and the half-times for the main kinetic phase for the mutant RCs increased in the order L162F, L162L, and L162G.

In a second set of experiments, excess cyt c_2 (cyt c_2:RC ratio = 6.5) was used. Again, the absorbance change at 1250 nm was recorded as in the experiments under equimolar conditions (Figure 1). The results for WT and a set of five mutant proteins are listed in Table I (columns 3 and 4). Only the L162F mutant showed a fast phase with an amplitude of 8%. Even under conditions where the fast phase was maximal for the WT [low detergent concentration (0.025% (w/v) LDAO), low ionic strength (<0.25 mM NaCl), and presence of a 10-fold excess of cyt c_2], no fast phase could be detected in any mutant RC except L162F. In this set of experiments using excess cyt c_2, L162M and L162S mutants were investigated, and the final order with respect to increasing half-times was found to be the same as that under equimolar conditions: Y(WT) < F < M < L < G < S.

From these experiments, it was concluded that the mutants can be separated into two groups: (1) the aromatic amino acid F at the position L162 results in a reorientation rate comparable to that in WT and may even permit a fast phase of electron transfer, however at the limit of detection; (2) the aliphatic residues at L162 result in slowed P^+ reduction kinetics. The phenomenon of rate increase upon the addition of excess cyt is discussed in more detail below (see also Figure 4).

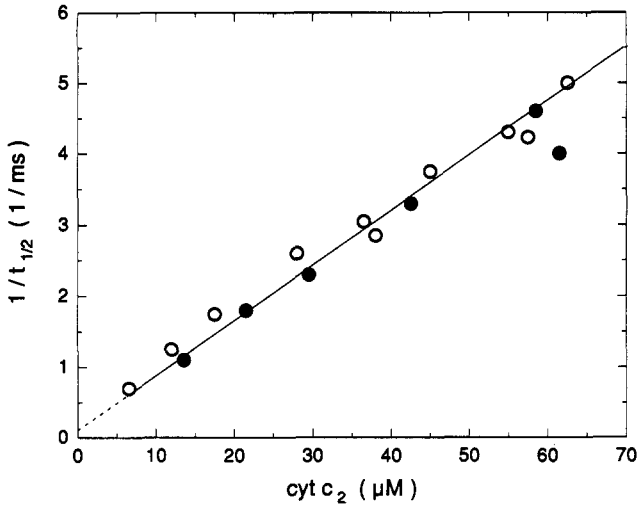

FIGURE 4: Cyt c_2 concentration dependence of the P^+ reduction and cyt oxidation kinetics in the L162G mutant. The reaction was measured at two different RC concentrations: 2.8 (○) and 11.3 μM (●).

Table II: Bimolecular Rate Constants (k_1) for the Cyt c_2–RC Association Reaction under Conditions of Excess Cyt[a]

	k_1 (10^8 M^{-1} s^{-1})	k_D (M)	k_{-1} (s^{-1})
WT	10.0	$\approx 10^{-6}$	$\approx 10^3$
L162F	4.7		
L162M	1.2		
L162L	1.1	$\approx 10^{-6}$	$\approx 10^2$
L162G	0.8		
L162S	0.5		

[a] The dissociation equilibrium constant (k_D) for WT RC and cyt c_2 is taken from Overfield et al. (1979); the competition experiment shown below indicates similar k_D values for WT and L162L RCs. The dissociation rate constant k_{-1} was calculated from k_1 and k_D. The kinetics of P^+ rereduction was tested by increasing the amounts of cyt c_2. RCs were present at 2 μM in 20 mM Tris (pH 8.0), 0.025% LDAO, 60 μM naphthoquinone, and 100 μM ascorbate.

Dependence of P^+ Rereduction Kinetics on Cyt Concentration. The experiments shown in Figures 1–3 were all performed under equimolar RC and cyt c_2 concentrations and were consistent with the minimal kinetic model shown above. However, when the cyt c_2 concentration was increased in excess of the RC, the observed kinetics changed drastically. When a 50-fold excess of cyt c_2 was added to the WT RC, the half-time of the fast phase did not change (0.8–1.0 μs), but the maximum amplitude was found to be as high as 80% of the signal (data not shown). The slow phase in WT as well as the kinetics observed for the mutants was accelerated to values far beyond the limit obtained by the measurements under equimolar conditions (Table I). This was demonstrated by adding additional amounts of cyt c_2 to an equimolar mixture of RC and cyt c_2, already at concentrations located on the plateau in Figure 3. The resulting increase of the observed rate (data not shown) was not consistent with the assumption of a pseudo-first-order plateau at concentrations of RC and cyt c_2 which would strongly favor the bound cyt c_2–RC complex state. It was concluded that an increasing cyt c_2 concentration had two effects on the kinetics: the rate of complex formation increased, and the rate-limiting reorientation step was accelerated. As a result, the bimolecular rate constants can be determined either from experiments, as shown in Figure 3, using the low concentration part of the curve or from experiments with constant RC and increasing cyt c_2 concentrations. The latter method is more accurate, and the rate constants obtained are summarized in Table II. The evaluation of the kinetic data for WT yielded a bimolecular rate constant of 1.0×10^9 M^{-1} s^{-1}, a value which compares well with the value of 6.4×10^8 M^{-1} s^{-1} obtained for low concentrations in Figure 3 and the previously published rate of 8.0×10^8 M^{-1} s^{-1} (Overfield et al., 1979), but is somewhat higher than the rate of 1.5×10^8 M^{-1} s^{-1} reported by Moser and Dutton (1988).

Given the current kinetic model, and the absence of a precise molecular interpretation of binding site(s), these results were interpreted in terms of a model by which excess cyt c_2 interacts with the RC in such a way that the velocity of the reorientation step increases with increasing cyt c_2 concentrations. Whether this excess also influences the affinity constants ($k_D^{(')} = k_{-1}^{(')}/k_1^{(')}$ is not known. It will later be discussed that the results found under the conditions of excess cyt c_2 are consistent with multiple binding sites for cyt c_2 on the RC. It is therefore important to state that the minimal reaction scheme shown above holds true only for equimolar reaction conditions, which were consequently applied for further experiments. This analysis was also assumed to be valid under substoichiometric conditions, where RC was in excess of cyt c_2 (see below).

All of the mutant RCs described here showed a similar acceleration effect upon the addition of cyt c_2. This was examined for two different RC concentrations for the L162G mutant (Figure 4). Measurements of this type were performed for all mutants, and the calculated bimolecular rate constants are summarized in Table II. The values show that one effect of the mutants was to slow the docking reaction (k_1); in the most extreme case, docking was slowed by a factor of 20. At the same time, it should be kept in mind that the P^+ decay rates differed by a factor of up to 1000 under conditions where complex formation was complete (as evidenced by the plateau in Figure 3). This suggested that the change in k_1 was only one of at least two independent mutational effects that had to be considered.

Light Intensity Dependence of the P^+ Reduction. As first demonstrated by van Grondelle et al. (1976), the mobility of cyt c_2 with respect to its binding to the RC can be tested with *in vitro* experiments by utilizing variable flash intensities and substoichiometric mixtures of cyt c_2 and RC. In the studies described here, the concentrations of RC and cyt c_2 were adjusted to 1 and 0.5 μM, respectively. The amount of P^+ formation (1 μM at the highest flash intensity) was reduced by progressive attenuation of the laser flash intensity, and the corresponding amount of cyt c_2 oxidation was measured 50 ms after the flash excitation. Single flash experiments showed that the (550–540 nm) kinetics reached a plateau on this time scale (data not shown), indicating that the reduction of RC by cyt c_2 was complete, and that in the presence of the exogenously added quinone there was no interference from the much slower $P^+Q^- \rightarrow PQ$ charge-recombination reaction (rate constant 0.5–1 s^{-1}; Clayton & Yau, 1972; Kleinfeld et al., 1984). The results for WT and L162F and L162G mutants are shown in Figure 5. The amounts of photooxidized RCs (detected at 540 nm) and oxidized cyt c_2 (550–540 nm) were recorded simultaneously. The theoretical prediction for an electron-transfer reaction within an RC–cyt c_2 complex is shown as a dotted line in Figure 5 and represents "immobile" cyt c_2. This curve would be expected if the rates of cyt exchange (k_{-1}' and k_1) were smaller than those of the intracomplex reactions (k_2 and k_3). The dashed line represents the predicted reaction for unbound or rapidly dissociating "mobile" cyt c_2.[2] The solid line was found to fit published data for the fast

[2] The term "mobile" is used here exclusively for association and dissociation phenomena of the macromolecules, not for rotational or translational measurements within this complex. Some degree of rotational or translational mobility of cyt c_2 within the complex therefore cannot be excluded, even if it looks immobile in this assay.

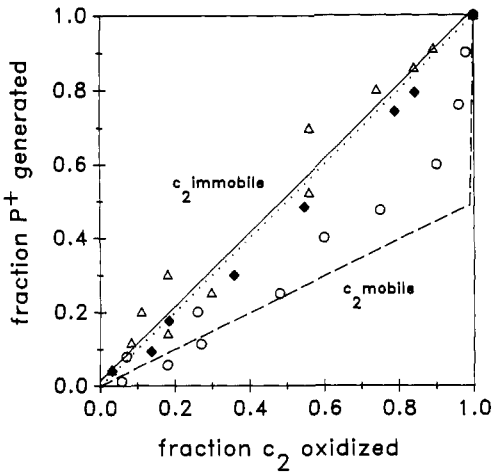

FIGURE 5: Light intensity dependence of P^+ rereduction. The unattenuated laser flash was able to photooxidize 100% of the RCs, which corresponds to a fraction of 1 on both axes. The flash intensity was decreased by neutral density filters, and the fractions of activated RCs (detected at 540 nm) and oxidized cyt c_2 (550–540 nm) were recorded simultaneously. The dotted and dashed lines represent the theoretical prediction for "immobile" and "mobile" cyt c_2, respectively. The solid line indicates the findings for the fast phase of WT RC reduction by cyt c (Overfield & Wraight, 1986). Symbols: slow phase in WT, ○; L162F, ◆; and L162G, △.

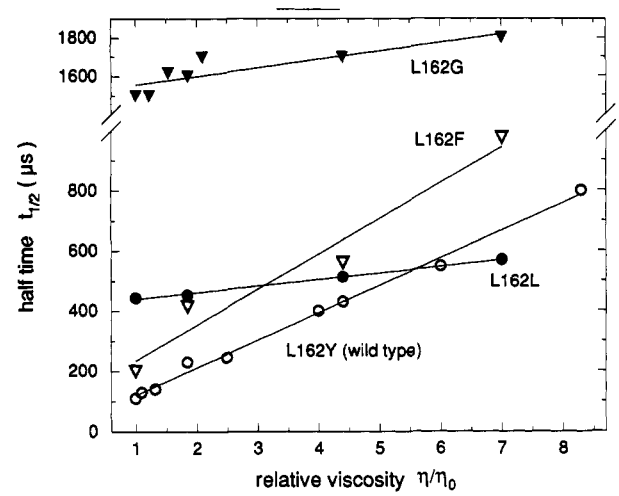

FIGURE 6: Effect of viscosity on the half-time of the P^+ reduction kinetics (for WT: slow component) at 1250 nm. The solutions contained equimolar amounts (10 μM) of reactants and increasing amounts of glycerol (max. 56%, which corresponds to $\eta/\eta_0 = 8.33$). The half-time dependence on the relative viscosity is linear, and the ratios of the slopes are WT:F:L:G = 1:1.3:0.24:0.47.

phase in WT RCs and cyt c (Overfield & Wright, 1986). Consistent with the observation of Moser and Dutton (1988), no such linear correlation between RC photooxidation and subsequent cyt c_2 oxidation was found here for the WT slow component (Figure 5). In our studies, flash intensities sufficient to photooxidize 60% of the RCs present resulted in the oxidation of 90% of the substoichiometric amount of cyt c_2 added. The slow phase of WT P^+ rereduction is thus attributable to cyt molecules which, within the time scale of the experiment, were not confined to a single RC. These cytochromes were able to diffuse to a photoactivated RC, even if they were previously bound to an RC that did not absorb a photon. Conversely, the fast phase of cyt oxidation depends linearly on the amount of P^+ produced, and therefore cyt exhibits no mobility on the time scale of the rapid electron-transfer reaction (Overfield & Wright, 1986).

The same types of experiments were carried out for the L162G mutant. The fraction of cyt c_2 oxidation was found to increase linearly with the extent of P^+ formation (Figure 5), just as described for the fast phase in WT. The L162F mutant basically showed the same behavior as the L162G mutant, although the data points systematically fell below the theoretical line for immobile cyt c_2. These results suggested that a change in k_{-2}', k_{-1}', or k_1 caused the decreased mobility of cyt c_2 in the mutants. An estimate of the dissociation rate for WT and the L162L mutant RC–cyt c_2 complexes is shown in Table II (column 3). A k_D value of 1.0 μM was found for the WT in equilibrium dialysis experiments (Rosen et al., 1980) and a similar value (1.1 μM) was measured in kinetic studies (Moser & Dutton, 1988). Since the competition experiment described here showed a similar affinity of the L162L RC for cyt c_2, the k_D value could not have been drastically altered in the mutants. The resulting k_{-1} value of 10^2 s^{-1} for L162L indicated that the dissociation rate in the mutants (especially for L162G) approached the measurement time of 50 ms, thereby explaining immobility on this time scale. Again, it must be pointed out that this partial saturation flash technique addressed the dissociation rate of reduced cyt from nonactivated RCs (k_{-1}'), whereas the k_{-1} value given above was that for the dissociation of a photooxidized RC–cyt c_2 complex. Given these facts, the explanation given above would only hold true when k_{-1}' and k_{-1} were identical or very similar. An alternative explanation for immobility and the observed values in the kinetics of the mutants would be a reduced reorientation rate (k_{-2}') relative to WT.

Viscosity Dependence of P^+ Rereduction. The electron-transfer step from cyt c_2 to RC occurs only from the tightly bound state and gives rise to the fast 1-μs kinetics seen in WT (Overfield et al., 1979). This kinetic component is independent of viscosity changes (P. Mathis, unpublished data). Since the slower phases are caused by incorrectly bound, or unbound, forms of cyt c_2, reorientation reactions and diffusional processes have to be performed prior to electron donation. It was reported earlier (Moser & Dutton, 1988) that these slower events in WT were viscosity-dependent and this was observed in our kinetic experiments, as shown in Figure 6. It was found that the rate of the slow rereduction process depended linearly on the relative viscosity, up to values of $\eta/\eta_0 = 8.33$ (56% glycerol). The L162F RCs showed viscosity-dependent kinetics in the sub-millisecond range, paralleling the findings for the slow phase of WT. The rereduction process in RCs with aliphatic substitutions was slow (see Figure 1 and Table I) and much less dependent on viscosity (shown in Figure 6 for L162G and L162L). Switching from an aqueous solution to 44% glycerol ($\eta/\eta_0 = 4.4$) increased the half-time in WT from 110 to 430 μs. In contrast, the half-time for L162L was much less sensitive to viscosity, increasing to 510 μs in 44% glycerol from 440 μs in aqueous solution. Regression analyses yielded the following equations for the viscosity-dependent behavior of the rates:

$$1/k = (28 + 91\eta/\eta_0)\ \mu s \quad \text{for WT}$$

$$1/k = (116 + 118\eta/\eta_0)\ \mu s \quad \text{for L162F}$$

$$1/k = (416 + 22\eta/\eta_0)\ \mu s \quad \text{for L162L}$$

$$1/k = (1512 + 43\eta/\eta_0)\ \mu s \quad \text{for L162G}$$

Since these experiments were carried out under conditions favoring complete complex formation, the results agree with a model that assumes slowed (Y → F) and drastically slowed (Y → L, S, M, G) electron transfer or reorientation instead of impaired docking. The assumption that the reorientation was affected in the mutants would imply that this step is much more viscosity dependent in WT and in the L162F mutant than in the L162L, -S, -M, and -G mutants.

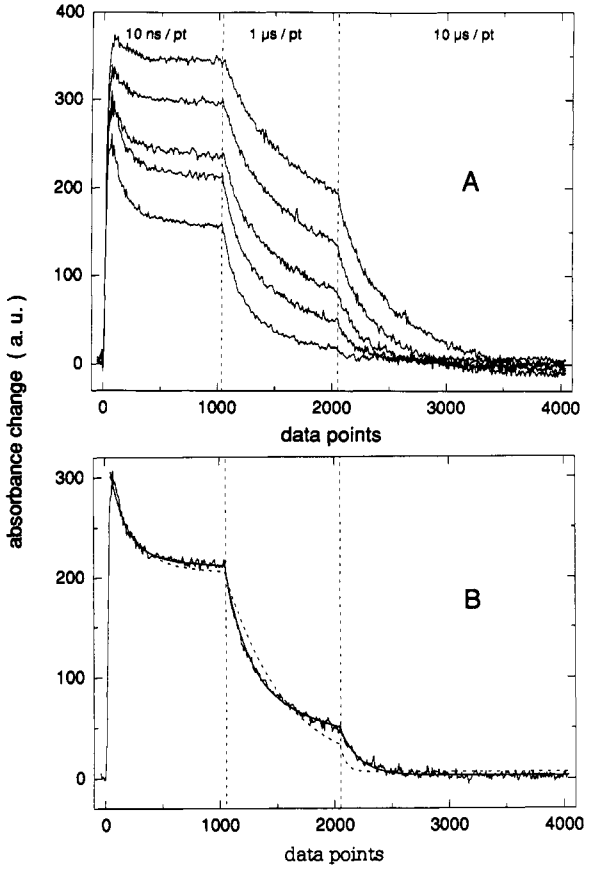

FIGURE 7: Competition experiment between WT and L162L RCs for cyt c_2. The traces for the L162L/WT RC ratios of 0, 0.3, 0.75, 1.35, and 3 (lower to upper curve) are shown in A [i.e., lower trace, WT RC alone (with equimolar amounts of cyt c_2, 10.2 μM); upper trace, 3-fold excess of L162L RCs]. B shows the best fit for low mutant RC concentration (RC ratio L162L:WT = 0.3) with two (- - -) or three (—) time constants. Rates and amplitudes of the fits are given in Table III.

Competition Experiments. Another series of experiments has been performed to examine further whether the binding between cyt c_2 and RC was altered in the mutants. Increasing amounts of L162L RCs were added to an equimolar (10 μM) solution of WT RC and cyt c_2, and the corresponding kinetics were recorded on three different time scales. Figure 7A shows the traces for different WT and L162L RC ratios. The addition of L162L RCs resulted in a reduction in the amplitude of the fast phase attributed to the WT RC–cyt c_2 complex and a concomitant increase in a slow phase characteristic for the L162L mutant. In contrast to the case where only WT RC and cyt c_2 were present (Figure 1), the kinetics of a WT/L162L mixture, even with no parameter constraints, could not be fit with two time constants, even at low concentrations of the L162L RC (Figure 7B). The introduction of a third (very slow) time constant, characteristic for the L162L reduction kinetics, yielded excellent agreement (Table III) between the modeled data and the measured kinetics (Figure 7B). Reasonable correlations were found for the ratio of the fit amplitudes assigned to the WT (fast and slow, columns 4 and 5) or the L162L (very slow, column 6) kinetics (column 10) and the ratio of the RC concentrations used in the experiment (column 3). The entire WT contribution (fast and slow phase) decreased upon L162L RC addition in a way that would be expected for comparable affinities of the two species for cyt c_2.

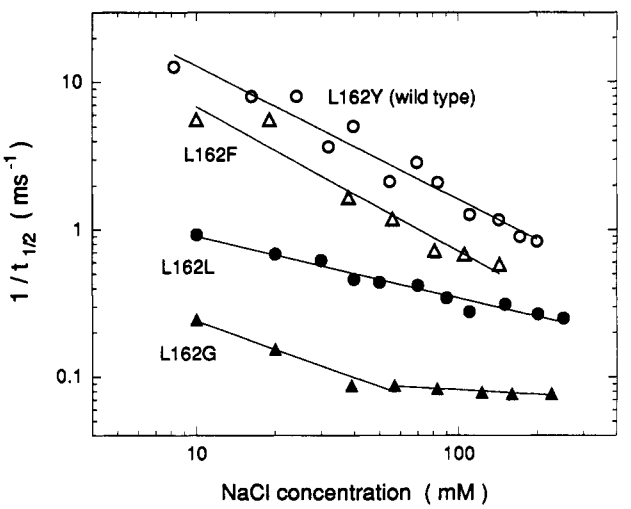

FIGURE 8: Double-logarithmic plot of the ionic strength dependence of the inverse half-time of the kinetics (slow part of WT kinetics). Conditions were as in Table I.

Ionic Strength Dependence. The dependence of the P^+ rereduction rate by cyt c_2 on increasing ionic strength is shown in Figure 8 for WT and L162F, L162L, and L162G. Inverse half-time rather than rate was plotted vs the salt concentration in Figure 8, since complex formation was prevented at high ionic strength making the process second-order. This was reflected clearly by the loss of fast phase amplitude in WT with increasing ionic strength. No fast phase was detected at salt concentrations above 100 mM. The experiments described here were limited to concentrations between 10 and 250 mM NaCl, and the case of very low salt concentrations was omitted since such conditions might lead to the formation of electrostatically stabilized complexes with multiple orientations between the redox partners not optimal for electron transfer (Hazzard et al., 1991).

In each case, a decrease in the electron-transfer rate with increasing ionic strength was observed. The slope of the curve was about the same for the WT and the L162F mutant (Figure 8), indicating comparable electrostatic interactions for these two cases. The ionic strength dependence of the mutant RCs L162L and L162G is much less pronounced (Figure 8), and the half-time of the L162G mutant did not change above 40 mM NaCl. This might indicate an upper limit for the P^+ lifetime, since at very slow cyt c_2 to RC electron-transfer rates the $P^+Q^- \rightarrow PQ$ charge recombination could compete for the

Table III: Quantitative Analysis of the Competition Experiment (Figure 7)[a]

[WT] (μM)	[L162L] (μM)	[WT]:[L162L] ratio	fast A_1/τ_1 (μs)	slow A_2/τ_2 (μs)	very slow A_3/τ_3 (ms)	$\sum A_i$ (i = 1–3)	A_1:($A_1 + A_2$) ratio	A_1:A_3 ratio	($A_1 + A_2$):A_3 ratio
10.2			132/1.6	153/150		285	0.46:1		
9.6	3.0	1:0.31	121/1.5	128/190	88/2.0	337	0.49:1	1:0.73	1:0.35
8.8	6.5	1:0.75	86.0/1.5	118/260	126/2.4	330	0.42:1	1:1.50	1:0.62
7.8	10.5	1:1.35	40.5/2.0	126/340	183/3.7	350	0.24:1	1:4.60	1:1.10
7.0	13.8	1:1.95	20.5/2.0	133/480	223/5.0	377	0.13:1	1:10.9	1:1.45

[a] Concentrations of WT and L162L RCs used in the competition experiment (columns 1 and 2); their ratios (column 3), fit amplitudes, and respective time constants (columns 4–6); and a comparison of the extent of fast phase and very slow phase in the fit (columns 7–9). Column 10 compares the amplitudes which are assigned to WT ($A_1 + A_2$) and mutant (A_3) contributions.

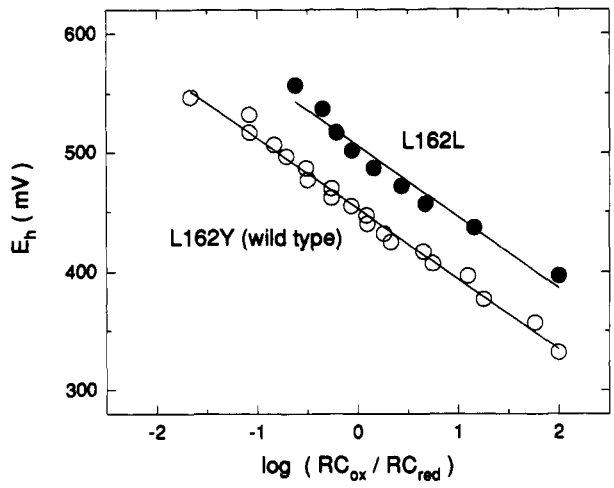

FIGURE 9: Nernst curve for the P/P^+ couple in WT (○) and L162L (●) RCs. The logarithm of the ratio of oxidized and reduced RC is plotted vs the ambient potential (E_h). The absorbance changes at 860 nm obtained from light-induced difference spectra were used. The corresponding midpoint potentials derived from the plot are $E_{m,8}^{WT}$ = 453 mV and $E_{m,8}^{L162L}$ = 506 mV.

Table IV: Electrochemical Redox Titration of L162 Mutant RCs[a]

	λ_{max} (nm)	$E_{m,8}$ (mV)	n
WT	863	453	1.0
L162F[b]	857	481	0.90
L162L	859	506	0.99
L162G	857	502	0.95

[a] The maximum of the P band (λ_{max}) was used for the evaluation of the midpoint potential. The n value was obtained in a linear regression procedure from the experimental data. The data represent averages of several independent titrations, i.e., two different RC preparations of the L162G mutant gave $E_{m,8}$ values of 501 (n = 0.9) and 503 mV (n = 1.0). [b] In a titration of L162F RCs reconstituted into liposomes, a midpoint potential $E_{m,8}$ of 495 mV was observed.

reduction of the dimer cation by cyt c_2. These results show that complex formation between cyt c_2 and RC is, to a large extent, electrostatically controlled and that the interaction is more favorable for WT and L162F than for the slower mutants L162L and L162G.

Electrochemical Redox Titration. Electrochemical redox titrations were carried out with WT and mutant RCs (Hawkridge & Ke, 1976) to determine whether the nature of the amino acid at position L162 influenced the midpoint potential of the P/P^+ couple. Light-minus-dark difference spectra for the Q_Y region (680–990 nm) of RCs during oxidative and reductive titrations were recorded for WT and mutants; the various applied potentials were controlled by a potentiostat. In each case, the following facts ensured the reliability of the titrations: (i) a stable isosbestic point was obtained at 798 nm; (ii) evaluation of the appearance/disappearance of the P band [at 855–866 nm, the position of this band varies with the substitution for L162Y (Farchaus et al., 1993)] or of the positive contribution of the electrochromic shift of the Q_Y band of B (at 782 nm) during a reductive/oxidative titration yielded the same result; (iii) the absence of hysteresis effects for oxidative and reductive steps proved the full reversibility of the titrations; (iv) the slopes of the corresponding Nernst curves (Figure 9) were close to −59 mV, indicative of single-electron (n = 1) redox reactions (Table IV).

Several complete titrations have been performed for WT, RCs, and an average midpoint potential $E_{m,8}$ of 453 mV (at pH 8 and 25 °C) was found. This value was in good agreement with the 450 mV values reported by Blankenship and Prince (1985), but somewhat lower than the 485 mV that was more recently measured in an ultra-thin-layer electrochemical cell (Moss et al., 1991). The midpoint potential of the P/P^+ couple was shifted in all mutants to more positive values. The "slow" mutants L162L and L162G, which showed the most drastic kinetic effects, also exhibited the largest shifts (≈50 mV) compared to WT, whereas the L162F mutant shift was intermediate. Figure 9 shows the Nernst curves for WT and the L162L mutant, and Table IV summarizes the results of the redox titrations of the P/P^+ couple.

L162F RCs were also incorporated into phospholipid liposomes, and the redox properties of the P/P^+ couple were again investigated. A midpoint potential $E_{m,8}$ of 495 mV was found, demonstrating that the mutations rather than the detergent solubilization of the RCs were likely the major determinant of the shift of $E_{m,8}$ (P/P^+) to more positive values.

Titration of native cyt c_2 revealed an $E_{m,7}$ of 348 mV (n = 1.0; data not shown), which was in very good agreement with the previously published value of 346 mV (Bartsch et al., 1971). This result indicated a larger E_m difference between the redox partners cyt $c_2^{(red)}$/cyt $c_2^{(ox)}$ and P/P^+ in the mutants than in WT. Experimental evidence for decreasing rate constants between redox partners with increasing free energy differences, $|\Delta G°|$, has been reported (Closs & Miller, 1988; Moore & Pettigrew, 1990). However, the magnitude of the E_m change was too small for the L162 mutants examined here by nearly an order of magnitude (Moser et al., 1992). The implications of E_m on the observed rates will be discussed in more detail later.

DISCUSSION

In this article, we present evidence for drastic changes in the cyt c_2 to RC electron-transfer *in vitro* upon substitution of L162Y with several other amino acids. These effects are in full agreement with the results obtained with intact chemoheterotrophically grown cells (Farchaus et al., 1993). The fast phase found in WT, which is indicative of a correctly bound and therefore rapidly donating cyt, is lost upon the replacement of L162Y. The half-time of the fast phase of electron donation seems to be somewhat shorter in solution at low ionic strength (0.8–1 μs) than in proteoliposomes (2 μs; Overfield & Wraight, 1980a; G. Venturoli, personal communication), chromatophores (3–4 μs; Overfield et al., 1979), and whole cells (3–6 μs; Farchaus et al., 1993). Since an increase in ionic strength decreases not only the extent of the fast phase but also its rate slightly (Overfield et al., 1979), the lower salt concentration used in most *in vitro* experiments could explain the difference in the fast kinetics.

In many studies, equine cyt c has been used instead of native cyt c_2, since both proteins have a similar folding pattern. The cyt c to RC electron-transfer reaction also shows biphasic behavior, but the rate of the fast reaction is 10 times slower than in the cyt c_2–RC system (Overfield & Wraight, 1980a; Long et al., 1989). For the description of the kinetic processes, even the same model as for the cyt c_2–RC interaction has been used. Yet the net charges at pH 8 are different [isoelectric points $pI^{cyt\ c}$ = 10.65, Ke et al. (1970); $pI^{cyt\ c_2}$ = 5.5, Meyer (1970)] and the redox midpoint potentials differ by 100 mV ($E_{m,7}^{cyt\ c}$ = 250 mV, $E_{m,7}^{cyt\ c_2}$ = 350 mV), and although the two cytochromes compete for the same binding site on the RC protein (Rosen et al., 1980), the heme orientation with respect to the membrane normal is tilted (7–8°) and rotated (32°) for the cyt c–RC complex compared to the cyt c_2–RC complex (Tiede, 1987). The different distribution of lysines on the surface of the two cytochromes may account for their different interactions with the RC, since electrostatic forces are a major determinant of these reactions (Hall et al., 1987). It can

therefore be argued that different thermodynamic and structural properties seem to be responsible for the variations seen in the two cases. For this reason, we have limited our studies to the analysis of native cyt c_2 to RC electron-transfer kinetics. The only exception was the cyt turnover experiment presented in the preceding article (Farchaus et al., 1993), which was performed with equine cyt *c*. Since the quinol/quinone exchange reaction at the Q_B site was the rate-limiting step in this experiment, the different type of cyt should not have affected the turnover rates. The WT and L162 mutants displayed similar rates of cyt oxidation, confirming the unaltered turnover activity of mutated RCs, which has also been reported for *Rhodobacter capsulatus* L162 mutants (Bylina et al., 1988).

In order to understand the kinetic effects seen in the mutants, the behavior in the WT strain ATCC 17023 had to be investigated. It was found that the experiments performed under equimolar conditions agreed reasonably well with previously published data (Overfield et al., 1979; Moser & Dutton, 1988). A three-state model (with states termed off, distal, and proximal) was required as a minimal model to describe correctly the complex kinetics of electron transfer from cyt c_2 to the photooxidized RC. At low ionic strength, the rate constants were found to be 1×10^9 M^{-1} s^{-1} for the second-order reaction, 1×10^4 s^{-1} for the distal/proximal reorientation, and 1×10^6 s^{-1} for the electron-transfer step.

In experiments in which the RC concentration was kept constant and the cyt c_2 concentration was increased, we found a linear increase in the rate of the slow phase, while the fast phase increased only in amplitude. The cyt dependence of the kinetics of the slow phase was expected if the concentrations of the reactants were low, since the process would then be second-order. This was in fact observed and reported in several cases in *R. sphaeroides* (Overfield & Wraight, 1980a; Moser & Dutton, 1988) and *R. capsulatus* (Venturoli et al., 1990). Deviations from the three-state model were found under these conditions of low substrate concentrations, and an additional "product inhibition" term was introduced that represented the competition of oxidized and reduced cyt for photooxidized RC (Moser & Dutton, 1988). However, it was surprising to find in our studies that the cyt dependence of the reaction persisted even at very high cyt c_2 concentrations and accelerated the slow phase of the reaction to values far beyond the apparent pseudo-first-order limit obtained in the equimolar experiments.

One explanation for these findings would require multiple cyt binding sites on the RC surface with different affinities. As the cyt concentration is increased, the low-affinity sites are filled. Since the reaction accelerates, a cyt bound to one of these sites would have to donate its electron faster than the cyt bound to the high-affinity site. If the distal state (RC···cyt c_2 in the model) consists of several different conformations of the RC—cyt c_2 complex, k_2 would not be a single rate constant, but rather a complex mixture, and the cyt dependence of the reorientation reaction would arise from that fact. This substrate-assisted reorientation rate is analogous to the situation described for the cyt *c*/cyt *c* peroxidase system (McLendon et al., 1993), where intracomplex rates were found to depend on the cyt *c* concentration. The question of how many cyt c_2 molecules are attached to each RC has been addressed in several studies, and answers have varied from a cyt c_2:RC ratio of 0.5 (Joliot et al., 1989), to 1 (Rosen et al., 1980; Bowyer et al., 1979), 2 (Dutton et al., 1975), or 3 (Pachence et al., 1983).

Attempts to model cyt docking also did not lead to a consistent picture. Two different binding sites were proposed: one directly above the bchl *a* dimer along the 2-fold symmetry axis (Allen et al., 1987) with a heme-to-dimer distance of 19 Å (measured from the iron to the magnesium), and another situated more on the M side of the RC surface (Tiede & Chang, 1988) with a center-to-center pigment distance of 23 Å. It was pointed out, however that several local energy minima were found in these calculations, which would be consistent with the existence of multiple binding sites of cyt c_2 on the RC protein. This would be in analogy to the biphasic redox reaction between cyt *c* and cyt oxidase, since in this system two cyt *c* molecules are bound with different affinities to a cyt oxidase monomer (Ferguson-Miller et al., 1978). Another interesting finding was the phospholipid dependence of the interaction between cyt and its oxidase, which again parallels the cyt c_2–RC system, wherein studies of neutral and negatively charged membranes revealed different kinetic results (Overfield & Wraight, 1980a,b). This might explain why a slow phase in the cyt c_2–RC reaction with a half-time much faster than 100 μs was seen only when solubilized RCs were investigated. Although the cyt concentration in the periplasmic space of intact cells can be as high as 1 mM (Prince et al., 1975) and a fast phase of electron donation can be detected, the half-time of the slow component is around 100 μs, the value of the pseudo-first-order plateau found in the equimolar experiments *in vitro* (Figure 3A and preceding article). It should be noted, however, that only under certain growth conditions does the amount of cyt c_2 exceed that of RC (Garcia et al., 1987) and that in semiaerobically grown cells the molar ratio of the two proteins should be close to 1, which means that the effect of excess cyt on the reorientation step might also be present in intact cells.

Two independent cyt c_2 binding sites with different affinities seem unlikely, since a linear increase of k_2 with cyt c_2 was found throughout the entire concentration range investigated here. In none of the cases (slow phase in WT or mutant kinetics) was a deviation from linearity observed. Therefore, it seems more likely that excess cyt mainly influences the rates of the reorientation step and to a minor extent also the equilibrium between the distal and the proximal states, favoring the proximal conformation. This can be seen from the fact that the amplitude of the 1-μs component, assigned to the rapidly donating proximal form, increases with cyt concentration (Table I; Long et al., 1989). If the cyt dependence of the reorientation steps (k_2 and to a lesser extent k_2') was assumed and introduced into the kinetic scheme, the extended three-state model could again account for the observed effects, since an increased k_2' would favor the proximal conformation in the dark and the amount of correctly bound cyt c_2 would be increased, resulting in a higher amplitude of the fast phase after photooxidation of the RC. An increase in k_2 as a function of cyt c_2 concentration would also ensure the acceleration of the distal to proximal reorientation reaction of cyt c_2 after flash activation.

All mutant RCs showed the same linear acceleration of the reaction rate upon cyt c_2 addition (Figure 4) as was found for the slow phase in WT. If the same reaction step was affected by excess cyt c_2 in the various RCs, the differences in electron-transfer kinetics in the mutants could be explained by differing reorientation rates. The loss of the fast phase would then be due to a shift in the distal/proximal equilibrium toward the nonproductively bound distal cyt c_2. In a simulation of this case, a decrease in the k_2':k_{-2}' ratio from 1 toward 0 would reduce (and finally remove) the amplitude of the fast phase of the reaction, leaving its rate unchanged. The remaining kinetics is dominated by the (cyt c_2-dependent) reorientation step and closely resembles the properties of the slow phase of WT RCs.

There are two other possibilities for display of the monophasic kinetics by the mutants in a simulation. First the cyt c_2 binding to RC could be drastically weakened in the mutants; therefore, even at high concentration of the reactants most of the cyt c_2 would be unbound, resulting in a second-order reaction with no observable fast phase. Second, if the electron-transfer step k_2 is slowed to values where it becomes rate-limiting, a monophasic P^+ decay would be observed regardless of the distal/proximal distribution. A slow k_3 requires the introduction of cyt c_2 dependence of the electron-transfer step to account for the results discussed above.

A drastic change in the dissociation constant ($k_D = k_{-1}/k_1$) seems an unlikely explanation for the observed impairment in the mutants if one considers that the change in the reaction order from second-order to pseudo-first-order and the pseudo-first-order plateau occur at similar concentrations for all RCs tested (Figure 3). A more direct comparison of cyt c_2 binding to WT and mutant RCs could be obtained in the competition experiment (Figure 7, Table III), where a similar affinity of WT and L162L RCs for cyt c_2 was found. Experiments with oriented samples are presently underway and investigate whether orientation, as well as binding of the docked cyt c_2, is conserved in the L162 mutants.

Since the association rate k_1 can be obtained from the measurements shown in Figures 3 and 4 and a value for k_D from the competition experiment (Figure 7), the dissociation rate k_{-1} can be calculated (Table II). Direct experimental evidence for a slower cyt c_2 dissociation from reduced RC (k_{-1}') is provided by the experiments using subsaturating excitation flashes of varying intensity (Figure 5). In these experiments, P^+ decay and cyt c_2 oxidation were recorded simultaneously. Since cyt c_2 was present in substoichiometric amounts, subsaturating flashes analyze the dissociation of unexcited RC–cyt c_2 and the formation of RC^+–cyt c_2 complexes within the limits of the observation time (50 ms). In order to obtain mobile cyt c_2 behavior, all of the rate constants involved have to be faster than the observation time. This is found for the slow component in WT. The finding that the WT curve lies well above the theoretical line expected for perfectly mobile cyt c_2 indicates that $1/k_{-1}'$ is close to the observation time of 50 ms. Immobile cyt c_2 in the L162G mutant indicated that, in this case, no productive new complex formation was possible within 50 ms. Since the P^+ decay is complete within 50 ms, if cyt c_2 is present in at least stoichiometric amounts (Tables I and II), the dissociation rate k_{-1}' must have been the rate-limiting step in the formation of a new complex. Slowing k_{-1}' by a factor of 10 (see Table II) would result in the immobile cyt c_2 observed for the L162G mutant. The L162F mutant represented an intermediate case, but it was somewhat surprising that cyt c_2 appeared rather immobile in this assay. Mobility is essential for the physiological function of cyt c_2, since its interaction domain is the same for the different redox partners (Margoliash & Bosshard, 1983; Hall et al., 1987). In the *in vivo* system, cyt c_2 oxidized by RC is subsequently reduced by the cyt bc_1 complex. As a consequence of the slow dissociation rate, this process should be slowed in the L162G mutant, explaining the impaired photoheterotrophic growth reported in the accompanying article.

It is widely accepted that the interaction between the RC and cyt c_2 is primarily electrostatically controlled. Although there are reports that indicate an involvement of the "back side" of cyt c_2 (i.e., the side opposite the heme crevice domain) in its docking to the RC in *Rhodospirillum rubrum* (Rieder et al., 1985), it is now well-established that the electron transfer in *R. sphaeroides* occurs via the solvent-exposed heme edge (Hall et al., 1987). Since the distribution of charged residues on the surface of the cyt c_2 molecule is highly asymmetric, the dipole moment is large and the heme crevice, which is surrounded by positively charged lysine residues, orients toward the negatively charged RC surface in a productive collision. The "initial docking" still allows rotation of the cyt c_2 molecule around its dipole axis and leads to multiple "distal" states. It is not surprising to find that the slow component of the WT kinetics, assigned to the distal state(s), exhibits no dichroic signal (Tiede, 1987). A certain pattern of negatively charged amino acid residues on the RC might energetically favor one (proximal) cyt c_2 position in which electron transfer would occur. This state is a defined complex and shows an oriented cyt c_2 molecule in the linear dichroism measurements (Tiede, 1987).

The view that the distal to proximal transition is a spatial (rotational or translational) reorientation was confirmed by the viscosity sensitivity of this reaction step (Moser & Dutton, 1988). We found a linear dependence of the rate on the relative viscosity in WT for both equimolar and excess cyt c_2 conditions, confirming again that the rate of this phase (k_2), but not its nature, was affected by increasing cyt c_2 concentrations. In the L162F mutant, the rate of the P^+ decay was similar to the rate of the slow first-order reaction in WT and also the viscosity sensitivity was found to be quite similar (Figure 6). This analogy also holds for the ionic strength dependence of this process (Figure 8). It is important to note that the mutants which exhibit a large kinetic effect (L162L and L162G) are much more insensitive to variation of both viscosity and ionic strength (Figures 6 and 8).

Taken by itself, the effect of viscosity on the reaction kinetics makes it tempting to suggest that in the L162F mutant the electron-transfer step (k_3) is still fast and a preferentially populated distal state results in a high viscosity sensitivity and a lack of a fast phase. If the removal of the aromatic character of the residue at position L162 slows the electron-transfer step (k_3) by 2-3 orders of magnitude, the observed kinetics would consist of a viscosity-independent reaction (electron transfer, k_3) and a viscosity-dependent reaction (reorientation, k_2), resulting in a decreased overall viscosity sensitivity of the process. However, at high relative viscosity of the solution, the L162L mutant reacts even faster with cyt c_2 than the L162F mutant (Figure 6). This, as well as the altered ionic strength dependence, can hardly be explained by a change in k_3 alone, but makes the following interpretation more plausible.

As discussed above, the distal to proximal reorientation reaction, and the distribution between the two states, is the most sensitive process in the cyt c_2–RC interaction. Without a tyrosine at position L162, the equal distribution between the two states is lost and the distal conformation(s) is (are) favored. In the L162F mutant the nature of the reorientation process is conserved; therefore, the kinetic constants observed and their dependencies on ionic strength and viscosity variation closely resemble those of the slow phase in WT. Introduction of L or G at position L162 also affects the reaction type of the reorientation process, changing the rate (k_2) and its dependencies. It is important to point out that this assumption is sufficient to explain all data without the necessity of a slow k_3 in the L162L and L162G mutants. The effect of L162Y on the rate of electron donation to P^+ can be measured directly in site-specific mutants of *Rps. viridis* which have recently been constructed (Laussemair & Oesterhelt, 1992), since the tightly bound tetraheme cytochrome presumably excludes any reorientation or binding effects.

In contrast to the almost exclusive electrostatic control of the docking and reorientation processes, the rate of the electron-

transfer step is guided by the distance of the reacting components. The driving force of the process is represented by the difference in the free energies between donor and acceptor ($\Delta G°$) and the reorganization energy (λ) which is required for the distortion of the nuclear configuration from the reactant to the product equilibrium coordinates. Only recently, Moser et al. (1992) found the donor–acceptor distance to be the major determinant of intramolecular electron transfer, and a linear distance–rate relationship over 12 orders of magnitude was found. However, $\Delta G°$ (and λ) can modulate the electron-transfer rate over several orders of magnitude. The importance of $\Delta G°$ is demonstrated by the arrangement of electron carriers according to their midpoint redox potentials, which represents the major thermodynamic construction principle of any electron-transport chain. The optimal rate is obtained when $-\Delta G° = \lambda$ (maximum of the Marcus plot; Marcus, 1956). In the redox titration, we found a higher $E_{m,8}(P/P^+)$ value for the L162 mutants than in WT, resulting in a higher free energy difference ($\Delta G°$) for the reaction. If we assume the optimal electron-transfer rate for WT RC, an increase in $\Delta G°$ in the mutants would place the reaction in the "inverted region" ($-\Delta G° > \lambda$) of the Marcus plot, where a $\Delta G°$ increase leads to a decrease in rate. The finding that the L162F mutant exhibits the smallest $E_{m,8}$ change (Table IV) and the fastest reaction rate (Table I) would support this view. However, the shallowness of the $\Delta G°$ vs log k plots (Moser et al., 1992) indicates that an $E_{m,8}$ change of at least 0.5 V would be necessary to account for the observed changes in the kinetics of the slow mutants.

This fact, together with the cyt dependence of the kinetics, makes it more likely that the mutation at position L162 primarily affect the labile equilibrium between productively and nonproductively bound cyt c_2 rather than the electron-transfer rate alone.

ACKNOWLEDGMENT

The authors thank W. Barz and J. Shiozawa for many stimulating discussions and critical reading of the manuscript.

REFERENCES

Bartsch, R. G. (1971) *Methods Enzymol. 23*, 344–363.
Blankenship, R. E., & Prince, R. C. (1985) *Trends Biochem. Sci. 10*, 382–383.
Bowyer, J. R., Tierney, G. V., & Crofts, A. R. (1979) *FEBS Lett. 101*, 207–212.
Bylina, E. J., Jovine, R., & Youvan, D. C. (1988) in *The Photosynthetic Bacterial Reaction Center, Structure and Dynamics* (Breton, J., & Verméglio, A., Eds.) pp 113–118, Plenum Press, New York.
Clayton, R. K., & Yau, H. F. (1972) *Biophys. J. 12*, 867–881.
Closs, G. L., & Miller, J. R. (1988) *Science 240*, 440–446.
Dutton, P. L., Petty, K. M., Bonner, H. S., & Morse, S. D. (1975) *Biochim. Biophys. Acta 387*, 536–556.
Farchaus, J. W., & Oesterhelt, D. (1989) *EMBO J. 8*, 47–54.
Farchaus, J. W., Grünberg, H., Gray, K. A., Wachtveitl, J., DeHoff, B., Kaplan, S., & Oesterhelt, D. (1990) in *Molecular biology of membrane-bound complexes in photosynthetic bacteria* (Drews, G., Ed.) pp 65–76, Plenum Press, London.
Farchaus, J. W., Wachtveitl, J., Mathis, P., & Oesterhelt, D. (1993) *Biochemistry 32*, preceding article in this issue.
Ferguson-Miller, S., Brautigan, D. L., & Margoliash, E. (1978) *J. Biol. Chem. 387*, 149–159.
Gabellini, N., Gao, Z., Oesterhelt, D., Venturoli, G., & Melandri, B. A. (1989) *Biochim. Biophys. Acta 974*, 202–210.
Garcia, A. F., Venturoli, G., Gad'on, N., Fernandez-Velasco, J. G., Melandri, B. A., & Drews, G. (1987) *Biochim. Biophys. Acta 890*, 335–345.
Gray, K. A., Farchaus, J. W., Wachtveitl, J., Breton, J., & Oesterhelt, D. (1990) *EMBO J. 9*, 2061–2070.
Hall, J., Zha, X., Yu, L., Yu, C. A., & Millet, F. (1987) *Biochemistry 26*, 4501–4504.
Hawkridge, F. M., & Ke, B. (1976) *Anal. Biochem. 78*, 76–85.
Hazzard, J. T., Rong, S., & Tollin, G. (1991) *Biochemistry 30*, 213–222.
Isied, S. S. (1984) *Prog. Inorg. Chem. 32*, 443–517.
Joliot, P., Verméglio, A., & Joliot, A. (1989) *Biochim. Biophys. Acta 975*, 336–345.
Ke, B., Chaney, T. H., & Reed, D. W. (1970) *Biochim. Biophys. Acta 216*, 373–383.
Kleinfeld, D., Okamura, M. Y., & Feher, G. (1984) *Biochim. Biophys. Acta 766*, 126–140.
Laussermair, E., & Oesterhelt, D. (1992) *EMBO J. 11*, 777–783.
Long, J. E., Durham, B., Okamura, M., & Millet, F. (1989) *Biochemistry 28*, 6970–6974.
Marcus, R. A. (1956) *J. Chem. Phys. 24*, 966–978.
Margoliash, E., & Bosshard, H. R. (1983) *Trends Biochem. Sci. 8*, 316–320.
Meyer, T. E. (1970) Ph.D. Thesis, University of California at San Diego, San Diego, CA.
Moore, G. R., & Pettigrew, G. W. (1990) in *Cytochromes c, Evolutonary, Structural and Physicochemical Aspects*, pp 363–408, Springer, Berlin.
Moser, C. C., & Dutton, P. L. (1988) *Biochemistry 27*, 2450–2461.
Moser, C. C., Keske, J. M., Warncke, K., Farid, R. S., & Dutton, P. L. (1992) *Nature 355*, 796–802.
Moss, D. A., Bauscher, L. M., & Mäntele, W. (1991) *FEBS Lett. 283*, 33–36.
Overfield, R. E., & Wraight, C. A. (1980a) *Biochemistry 19*, 3322–3327.
Overfield, R. E., & Wraight, C. A. (1980b) *Biochemistry 19*, 3328–3334.
Overfield, R. E., & Wraight, C. A. & DeVault, D. (1979) *FEBS Lett. 105*, 137–142.
Pachence, J. M., Dutton, P. L., & Blasie, J. K. (1983) *Biochim. Biophys. Acta 724*, 6–19.
Prince, R. C., Cogdell, R. J., & Crofts, A. R. (1974) *Biochim. Biophys. Acta 347*, 1–13.
Prince, R. C., Baccarini-Melandri, A., Hauska, G. A., Melandri, B. A., & Crofts, A. R. (1975) *Biochim. Biophys. Acta 387*, 212–227.
Rosen, D., Okamura, M. Y., & Feher, G. (1980) *Biochemistry 19*, 5687–5692.
Smith, J. M., Smith, W. H., & Knaff, D. B. (1981) *Biochim. Biophys. Acta 635*, 405–411.
Tiede, D. M. (1987) *Biochemistry 26*, 397–410.
Tiede, D. M., & Chang, C. H. (1988) *Isr. J. Chem. 28*, 183–191.
Tiede, D. M., Vashishta, A.-C., & Gunner, M. R. (1993) *Biochemistry 32*, 4515–4531.
Van der Wal, H. N., Van Grondelle, R., Millet, F., & Knaff, D. B. (1987) *Biochim. Biophys. Acta 893*, 490–498.
Van Grondelle, R., Duysens, L. N. M., & Van der Wal, H. N. (1976) *Biochim. Biophys. Acta 449*, 169–187.
Venturoli, G., Melandri, B. A., Gabellini, N., & Oesterhelt, D. (1990) *Eur. J. Biochem. 189*, 105–112.
Wachtveitl, J., Laussermair, E., Mathis, P., Farchaus, J. W., & Oesterhelt, D. (1993) *Biochem. Soc. Trans. 21/1*, 43–44.